Neurobiology of Aging 43 (2016) 13–22

Contents lists available at ScienceDirect

Neurobiology of Aging

journal homepage: www.elsevier.com/locate/neuaging

Differential effects of *Cdh23*^{753A} on auditory and vestibular functional aging in C57BL/6J mice

Bruce E. Mock [1], Sarath Vijayakumar [2], Jessica Pierce, Timothy A. Jones [2], Sherri M. Jones*,[2]

Department of Communication Sciences and Disorders, East Carolina University, Greenville, NC, USA

ARTICLE INFO

Article history:
Received 9 October 2015
Received in revised form 4 February 2016
Accepted 13 March 2016
Available online 26 March 2016

Keywords:
Utricle
Saccule
Cochlea
Vestibular
Auditory
Hearing
Balance
Aging

ABSTRACT

The C57BL/6J (B6) mouse strain carries a cadherin 23 mutation (*Cdh23*^{753A}, also known as *Ahl*), which affects inner ear structures and results in age-related hearing loss. The B6.CAST strain harbors the wild type *Cdh23* gene, and hence, the influence of *Ahl* is absent. The purpose of the present study was to characterize the effect of age and gender on gravity receptor function in B6 and B6.CAST strains and to compare functional aging between auditory and vestibular modalities. Auditory sensitivity declined at significantly faster rates than gravity receptor sensitivity for both strains. Indeed, vestibular functional aging was minimal for both strains. The comparatively smaller loss of macular versus cochlear sensitivity in both the B6 and B6.CAST strains suggests that the contribution of *Ahl* to the aging of the vestibular system is minimal, and thus very different than its influence on aging of the auditory system. Alternatively, there exist unidentified genes or gene modifiers that serve to slow the degeneration of gravity receptor structures and maintain gravity receptor sensitivity into advanced age.

1. Introduction

The inner ear houses the sensory organs for hearing and balance. Dysfunction in any of the inner ear end organs or their central pathways can cause hearing and/or vestibular impairment. Age-related hearing loss (ARHL) is the most common type of hearing impairment in humans, affecting 50% of the population by age 80 (Gorlin et al., 1995; Morton, 1991). The anatomical and physiological mechanisms of auditory aging have been extensively studied in both humans and animal models. However, relatively little has been done to investigate the role of age and predisposing factors (such as gender and genetic background) on vestibular function in spite of evidence that 3.4% of the US adult population (6.2 million people) suffers from chronic dizziness and/or imbalance (Hoffman and Sklare, 2003), 24% of people older than 72 years in the United States have suffered an episode of dizziness lasting for at least a month (Tinetti et al., 2000), 30% of people older than 65 years in the UK have dizziness (Colledge et al., 1994) and as many as 7 million people per year seek care for disequilibrium and/or vertigo.

Studies of the effect of age on vestibular function have typically used indirect measures such as the vestibulo-ocular reflex (VOR), optokinetic response, the otolith-ocular reflex, visual-vestibular responses, and tests of posture to infer peripheral vestibular status (Baloh et al., 1993; Enrietto et al., 1999; Furman and Redfern, 2001; Goebel, 2001; Paige, 1992, 1994; Shiga et al., 2005). Reported findings include decreased VOR gain, increased phase lead, decreased ability to suppress VOR with vision, less shortening of the VOR time constant by postrotary head tilt, and lower optokinetic response slow-phase velocity saturation.

Studies using a direct measure of peripheral vestibular function (vestibular sensory evoked potentials [VsEPs]), in a variety of inbred mouse strains, highlight the importance of genetic background for gravity receptor function (e.g., Jones et al., 2005, 2006). Furthermore, these studies suggest that a genetic predisposition for a functional deficit in one inner ear sensory modality does not obligate functional loss in the other modality (e.g., Jones et al., 2005, 2006; Lee et al., 2013; Zhao et al., 2008).

The C57BL/6J (B6) mouse has been extensively studied and is a well-established model for ARHL (Bartolome et al., 2002; Henry, 2002; Hequembourg and Liberman, 2001; Johnson et al., 1997;

* Corresponding author at: Department of Special Education and Communication Disorders, University of Nebraska-Lincoln, 301 Barkley Memorial Center, Lincoln, NE, 68583-0738, USA. Tel.: (402) 472 5496; fax: (402) 472 7697.
E-mail address: sherri.jones@unl.edu (S.M. Jones).
[1] Present Address: Veterans Administration Hospital, 1705 Gardner Road, Wilmington, NC 28405.
[2] Present Address: Department of Special Education and Communication Disorders, University of Nebraska-Lincoln, Lincoln, NE 68583.

0197-4580/$ – see front matter © 2016 Elsevier Inc. All rights reserved.
http://dx.doi.org/10.1016/j.neurobiolaging.2016.03.013

McFadden et al., 2001; Spongr et al., 1997). To date, at least 10 quantitative trait loci that contribute to ARHL have been identified in mice (Latoche et al., 2011; Noben-Trauth and Johnson, 2009). The *Ahl* mutation (also known as *Cdh23*^{753A}) was the first mutation discovered in association with ARHL and appears to be the most common ARHL mutation (Johnson et al., 1997; Noben-Trauth et al., 2003). *Ahl* is a recessive, single nucleotide mutation at 753 (G≥A) on the *Cdh23* gene on mouse chromosome 10 (Noben-Trauth et al., 2003). *Cdh23* encodes cadherin 23, a protein necessary for inner ear development and maintenance of sensory cell structures such as stereociliary tip links (Kazmierczak et al., 2007; Siemens et al., 2004; Söllner et al., 2004) kinocilial and transient lateral links (Lagziel et al., 2005; Michel et al., 2005).

The effects of the *Ahl* mutation on vestibular structure and function are not well understood. The purpose of the present study was to evaluate whether the *Ahl* mutation, which when homozygous produces profound loss of hearing with age, has a similar effect on inner ear vestibular function. We characterized the effect of age and gender on macular function in B6 mice harboring the *Ahl* mutation and an inbred congenic strain, B6.CAST-*Cdh23*$^{Ahl+/Kjn}$ (B6.CAST), that is genetically identical to the B6 strain except for a small region of Chromosome 10 inherited from the CAST/Ei strain that contains the *Ahl* locus (Johnson et al., 1997; Keithley et al., 2004). Thus, in the B6.CAST strain, the *Ahl* locus is replaced by the normal dominant wild-type allele that is resistant to ARHL. In the resistant B6.CAST strain, the progression of ARHL is delayed by about 3–6 months and attenuated compared to B6 (Keithley et al., 2004).

The main objectives of the present study were to address the following questions: (1) are there differences in age-related decline of auditory and gravity receptor function and are there gender differences in functional decline; and (2) will elimination of the *Cdh23*^{753A} mutation confer protection and modify the vestibular aging profile? To answer these questions, we measured VsEPs to assess macular function and auditory brainstem responses (ABRs) to characterize auditory function in female and male B6 and B6.CAST mice. Confocal microscopic images of the utricle were quantitatively compared to determine if any age-related functional change in gravity receptor function might be explained by structural changes, especially synaptic morphology of sensory neuroepithelium.

2. Methods

2.1. Animals

Breeder pairs for C57BL/6J (stock #000664) and B6.CAST-*Cdh23*$^{Ahl+/Kjn}$ (stock #002756) were purchased from the Jackson Laboratory (Bar Harbor, ME, USA) and colonies of both strains were established at East Carolina University. Both sexes of B6 (n = 158, ages 1.02–23.8 months) and B6.CAST (n = 109, ages 2.1–24.5 months) were studied. Table 1 indicates the number of animals measured for ABR and VsEPs. Animals were housed in standard polyurethane cages grouped by gender within a temperature-regulated (21 + 3/−4 °C) room under routine 12-hour light and/or dark cycle with access to food and water ad libitum. Animal care and all procedures were approved by the Institutional Animal Care and Use Committee and met NIH guidelines for the care and use of laboratory animals.

Table 1
Number of data points for each threshold measure

Strain	8 kHz	16 kHz	32 kHz	41.2 kHz	VsEP
B6	75 females	75 females	73 female	74 female	68 females
	75 males	74 males	75 male	75 males	71 males
	150 total	149 total	148 total	149 total	139 total
B6.CAST	31 female	31 female	31 female	30 female	49 female
	42 male	40 male	38 male	38 male	55 male
	73 total	71 total	69 total	68 total	104 total

The table indicates the number of mice tested for each measure and includes cases where the measurement was performed but there was no measurable response (no response).
Key: VsEP, vestibular sensory evoked potentials.

Ambient noise levels in the animal housing area were monitored throughout the study to assure that noise levels were below those which might result in noise-induced hearing loss. The ambient sound exposure levels for animals in laboratory housing areas were estimated using a data logging dosimeter. Forty-eight noise samples, each comprised of 16-hour periods were taken on randomly chosen days over a 5-month period. Logged data were discretized into mean sound pressure level (SPL) for each 10-minute period of recording. The logger had a sound floor of 65 dB SPL, so all levels below that were given a value of 65 dB SPL. The mean ambient level across all logs was 66.8 dB SPL. One 10-minute period registered 85 dB SPL and was the maximum level recorded. Six 10-minute periods were between 75 and 80 dB SPL. Thirty-three periods were between 70 and 75 dB SPL, whereas the remaining 4568 ten-minute periods were below 70 dB SPL.

2.2. Functional assessment of vestibular and auditory sensors

Animal preparation and functional testing for VsEPs and ABR followed procedures described by Mock et al. (2011) and Vijayakumar et al. (2015). Briefly, mice were anesthetized with a ketamine (18 mg/mL) and xylazine (2 mg/mL) solution (5–9 μL/g body weight injected intraperitoneally). Core body temperature was maintained at 37.0 ± 0.1 °C. Linear acceleration pulses, 2-ms duration, were presented to the cranium via a noninvasive spring clip that encircled the head anterior to the pinna and secured the head to a voltage-controlled mechanical shaker. Stimuli were presented along the naso-occipital axis at a rate of 17 pulses/sec. Stimulus amplitude ranged from +6 dB to −18 dB re: 1.0 g/ms (where 1 g = 9.8 m/s^2) adjusted in 3 dB steps. Stainless steel wire was placed subcutaneously at the nuchal crest to serve as the noninverting electrode. Needle electrodes were placed posterior to the left pinna and at the hip for inverting and ground electrodes, respectively. Traditional signal averaging was used to resolve responses in electrophysiological recordings. Ongoing electroencephalographic activity was amplified (200,000X), filtered (300–3000 Hz), and digitized (100-kHz sampling rate). Two hundred fifty-six primary responses were averaged for each VsEP response waveform. All responses were replicated. A broad band forward masker (50–50,000 Hz, 94 dB SPL) was presented during VsEP measurements to verify absence of cochlear responses.

For ABR measurements, pure tone burst stimuli were generated and controlled using National Instruments data acquisition system and custom software. Tone bursts at 8, 16, and 32 kHz, 41.2 kHz had 1.0-ms rise and fall times with 1.0-ms plateau (3-ms total duration). Stimuli for ABR testing were calibrated using a Bruel & Kjaar ¼ inch microphone and Nexus amplifier. Stimuli were calibrated in dB peak equivalent SPL (peSPL) and were presented via high frequency transducers (ED1 driver, EC1 speakers, Tucker–Davis Technologies) coupled at the left ear via a modified commercial ear tip (ER 10D-T03, Etymotic Research, Inc). Auditory stimuli were presented at a rate of 17 stimuli/s. ABR intensity series were collected by reducing the stimulus in 10-dB steps at higher stimulus levels and 5-dB steps closer to threshold. At the end of functional testing, mice were euthanized, and temporal bones were dissected for immunohistochemistry and confocal microscopy.

2.3. Fluorescent immunostaining and image analysis

Temporal bones were dissected from mice representative of young (3–6 months), mid (10–12 months), old (15–18 months), and very-old (22–24 months) age groups. In each age group, samples from at least 3 animals were examined. Oval and round windows were opened, and the apex of the cochlea was broken to allow permeation of the fixative (4% paraformaldehyde in 0.1-M phosphate buffer pH 7.4) overnight at 4 °C. The following day fixed, nondecalcified temporal bones were transferred to a petri dish containing ice-cold phosphate-buffered saline (PBS, pH 7.4). With the medial side facing up, the bony shelf of the labyrinth was removed to expose the pigmented roof epithelium overlying the utricle. The pigmented epithelium was then carefully removed, and otoconia covering the utricle were gently scraped off using a no.1 superfine eyelash brush (Ted Pella, Inc, Redding, CA). The utricle along with anterior and horizontal cristae of the semicircular canals was pulled out from the bony labyrinth and transferred to fresh PBS in a multiwell plate. Samples were washed 3 times in PBS for 10 minutes each, and then incubated in PBS containing 0.3% Triton X-100% and 10% normal goat serum (Vector Labs, Burlingame, CA) overnight at 4 °C to block nonspecific background labeling. After the block, samples were incubated with primary antibodies at 4 °C for 36–48 hours and subsequently washed in 0.3% PBS-Triton-X for 3x10 minutes. Samples were then incubated with secondary antibody cocktail overnight at 4 °C followed by 3 washes in PBS-Triton-X. The following primary antibodies were used: polyclonal rabbit anti-SHANK1 (1:300; Neuromics, Minneapolis, MN, USA), monoclonal mouse anti-CtBP2 (1:200; BD Biosciences, San Jose, CA, USA), polyclonal guinea pig anti-LHX3 (1:1000; gifted by Dr. Samuel L Pfaff, Salk Institute, La Jolla, CA, USA). The secondary antibodies used were Alexa Fluor 633 labeled goat anti-rabbit IgG antibody, Alexa Fluor 488 labeled goat anti-mouse IgG antibody, and Alexa Fluor 546 labeled goat anti-guinea pig (1:200; Invitrogen, Grand Island, NY, USA). The samples were then washed 3 times in PBS for 10 minutes each and mounted in ProLong Gold (Invitrogen) antifade mounting medium and coverslipped on Superfrost Plus slide (Fisher Scientific, Pittsburgh, PA, USA). Specificities of the antibodies were evaluated by preadsorption of the antibodies with the specific blocking peptides.

Whole mounts of the utricles were viewed and images were acquired on a laser scanning confocal microscope, LSM 510 (Carl Zeiss AG, Germany) using 100× oil-immersion objective (N.A 1.3) at 2× digital zoom. *z*-stacks were acquired at 1024 × 1024 raster (x and $y = 0.045$ μm, *z*-step = 0.14 μm). To minimize variation across samples, detector gain and excitation thresholds were adjusted for the same level of pixel saturation. Each *z*-stack contained the entire synaptic pole of the hair cell. Images were analyzed offline on Volocity 3D Image Analysis software (PerkinElmer, Waltham, MA, USA). All images were analyzed by 3 individuals blind to the age group. Hair cells and synaptic ribbons were counted manually employing C-terminal binding protein 2 (CtBP2) as the marker (Khimich et al., 2005; Liberman et al., 2011). Postsynaptic receptor patches were counted automatically using SHANK1 as the marker and expressed in terms of puncta per *z*-stack volume (Braude et al., 2015; Mendus et al., 2014). CtBP2-labeled hair cell nuclei were followed through the *z*-stack and were spot marked in the software to avoid double counting. Some samples were also immunolabeled for CtBP2 and LHX3, a transcription factor that is hair cell specific (Hume et al., 2007; Sage et al., 2005). LHX3 labeling helped in differentiating hair cell nuclei from supporting cell nuclei. CtBP2 and SHANK1a puncta counts were initially expressed as per *z*-stack volume and are reported as per hair cell in the results. Several metrics were characterized as follows: Hair cell density was calculated as the number of hair cells per scan field area of 2025 μm^2. Synaptic ribbon density was estimated as the number of CtBP2-immunolabeled puncta per hair cell. Postsynaptic marker density was estimated as the number of SHANK1a-stained puncta per hair cell. Synapses were identified as co-localized pre- and postsynaptic markers of CtBP2 and SHANK1a puncta, respectively.

2.4. Data analysis

The activity of the peripheral vestibular nerve has been shown to be reflected by the first 2 response peaks of the VsEP (P1, N1, Nazareth and Jones, 1998). Therefore, amplitude and latency measures for the first response peaks (P1 and N1) of the waveform were quantified. Threshold was defined as the intensity midway between the minimum stimulus intensity that produced a discernible response and the maximum stimulus intensity that did not result in a visible response. Response peak latency was defined as the time, in microseconds (μs), from onset of the stimulus to the appearance of P1. Peak-to-peak amplitude, (P1-N1) measured in microvolts (μV), represented the difference between each positive peak and its respective negative peak.

In cases where animals evidenced no response to testing at any stimulus level, the animals were scored as “no response” (NR). We characterized the percent of NR animals (% NR) at any given age period by ordering the list of animals by age, noting the number of nonresponding animals in each possible contiguous group of 10 animals in the list, dividing each by 10 to obtain the fraction and multiplying by 100 to obtain percent. Thus, the first 10 animals of the list (1–10) generates the first % NR, the second group (animals 2–11) the second % NR and so on until the end of the list is reached. The age representing each group was taken to be the age of the oldest animal in the group of 10 animals. An animal that has no response is distinguished from an animal where testing was not competed, in which case no data were entered.

For comparing cochlear and gravity receptor sensitivity, ABR and VsEP thresholds were normalized to represent a percent change in the dynamic range (% deficit) as described previously (Mock et al., 2011). The upper limit for ABR dynamic range was set to 100-dB peSPL, representing the highest level not producing temporary threshold shift as determined previously (Mock, 2008; Mock et al., 2011). The lower limit for the dynamic range was set to the lowest threshold obtained for each test frequency and strain. For B6 mice, the lowest threshold obtained for 8, 16, 32, and 41.2-kHz was 18.9, 7.9, 4.9, and 27.3-dB peSPL, respectively. Whereas for the B6.CAST, the lowest thresholds obtained were 25.9, 21.1, 10.8, and 10.9-dB peSPL across the test frequencies. For VsEPs, the lowest thresholds measured were −16.5 dB re: 1.0 g/ms for both B6 and B6.CAST mice. The maximum non-noxious stimulus level presented for VsEPs was +6 dB re: 1.0 g/ms.

2.5. Statistics

Linear regression and univariate or multivariate analysis of variance (Regression, ANOVA, MANOVA, respectively; SPSS, v22, IL) were used to evaluate auditory and gravity receptor function across age. For post hoc analysis, the least significant difference test was used. Linear regression was used to test relationships between response metrics (i.e., latency, amplitude, and threshold) and age and to determine the corresponding regression coefficients for rate of aging (slope) and intercept. A value of 110-dB peSPL was assigned for ABR threshold when responses were absent. In the case where there were no responses from any animal above a particular age, regression analysis (metric versus age) was restricted to ages where responses were present. To compare linear regression slopes, a macro (Dong, 2005, distributed by Infoclearinghouse.com) for MINITAB (v17, PA) based on Zar’s student’s *t* test (Zar-*t*, Zar, 1984)

was used. Unless stated specifically, data are presented as mean ± standard deviation (sample size). The criterion for statistical significance was $p < 0.05$.

3. Results

3.1. Effects of gender

For B6 mice, there were no significant differences in aging rates (rate of change per month) between males and females for any metric used to analyze vestibular and auditory measurements. Similarly, aging rates for vestibular latencies (P1) and thresholds as well as 8-kHz ABR thresholds indicated no gender difference in B6.CAST mice. However, gender differences were indicated for aging of VsEP amplitudes (P1-N1) and ABR thresholds for frequencies above 8-kHz in B6.CAST mice. In cases where there were no differences between genders, data for males and females were pooled for further analysis. In B6.CAST where gender differences were observed, data for each gender were evaluated separately. Fig. 1 illustrates VsEP thresholds for males and females of both strains (B6 and B6.CAST) and Fig. 2 summarizes findings for 8-kHz ABR thresholds for each gender. Regression lines shown in Figs. 1 and 2 represent combined male and female data. Interestingly, although

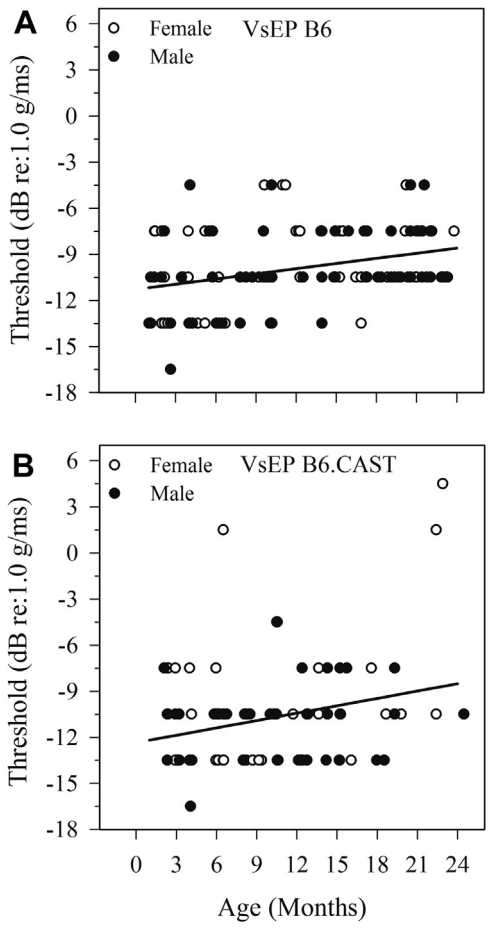

Fig. 1. VsEP thresholds as a function of age for male and female B6 (A) and B6.CAST (B) strains. Threshold increased with age for both strains. Linear regression lines (1 for each strain) reflect threshold aging rates for combined male and female data. No significant gender differences were found for slope or intercept for either strain. Regression lines, B6: y = 0.11x − 11.3 (dB re: 1.0 g/ms); B6.CAST: y = 0.16x − 12.4 (dB re: 1.0 g/ms). There was no significant difference in aging rates between strains. Abbreviation: VsEP, vestibular sensory evoked potentials.

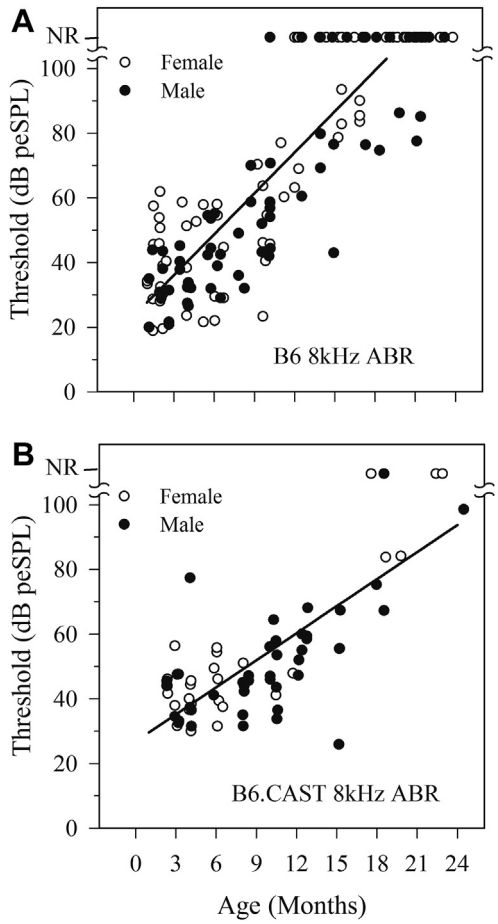

Fig. 2. ABR thresholds for 8-kHz stimuli as a function of age. Data for both male and female B6 (A) and B6.CAST (B) mice are shown. Linear regression equations reflect ABR 8-kHz threshold aging rates and are based on combined male and female data. There were no significant gender differences. Regression line equations: B6: y = 4.22x + 23.4 (dB SPL) and B6.CAST: y = 2.79x + 26.8 (dB SPL). The rate of increase in threshold with age for the B6 strain was significantly higher than the B6.CAST strain. Abbreviations: ABR, auditory brainstem responses; NR, no response; SPL, sound pressure level.

the aging rates for B6 males and females were the same for 8-kHz and 16-kHz ABR, thresholds were generally higher for females when age was taken into consideration as a covariate (ANOVA, 8 kHz: F[1,98] = 5.190, $p = 0.025$; 16 kHz: F[1,80] = 4.108, $p = 0.046$). The generally higher thresholds for females are thus independent of age and can be appreciated in Fig. 2A.

3.2. Age-related changes in gravity receptor function

VsEP responses were obtained for 139 B6 mice and 104 B6.CAST mice. VsEP thresholds were relatively stable across age for both strains, although both strains exhibited a shallow increase in threshold with age such that threshold increased by 0.11 dB per month for B6 mice (Fig. 1A, intercept = −11.28 dB re: 1.0 g/ms, F(1,137) = 14.46, $p = 2.15 \times 10^{-4}$, $R^2 = 0.095$) and 0.16-dB per month for B6.CAST (Fig. 1B, intercept = −12.355, F(1,102) = 7.94, $p = 0.006$, $R^2 = 0.072$). The aging slopes for threshold were not significantly different for the 2 strains, and there were no significant differences in threshold between strains when age was treated as a covariate. Age-related threshold changes corresponded on average to an increase in threshold of about 2.6 dB (B6) to 3.8 dB (B6.CAST) over the course of a lifetime (e.g., 24 months). Thus, the effect size (R^2) of age

on vestibular threshold was quite small for both B6 and B6.CAST mice.

VsEP onset latencies for P1 increased slightly and progressively with age for the B6 strain as can be seen in Fig. 3A (slope = 9.84 μs per month, intercept = 1270 μs, F(1,137) = 55.77, $p = 2.46 \times 10^{-8}$, $R^2 = 0.204$). In contrast there was no significant increase in onset latency with age in B6.CAST animals (slope = 1.524 μs per month, intercept = 1371 μs, F(1,102) = 0.945, p =0.333, $R^2 = 0.009$). Although aging latency slopes were significantly different between strains (Zar-*t*: $p < 0.05$), there was no general effect of strain on latency when age was taken into consideration (ANOVA, age as covariate). The age-related changes in latency for B6 mice represented very modest increases on average leading to response delays of about 240 μs over the period of a lifetime.

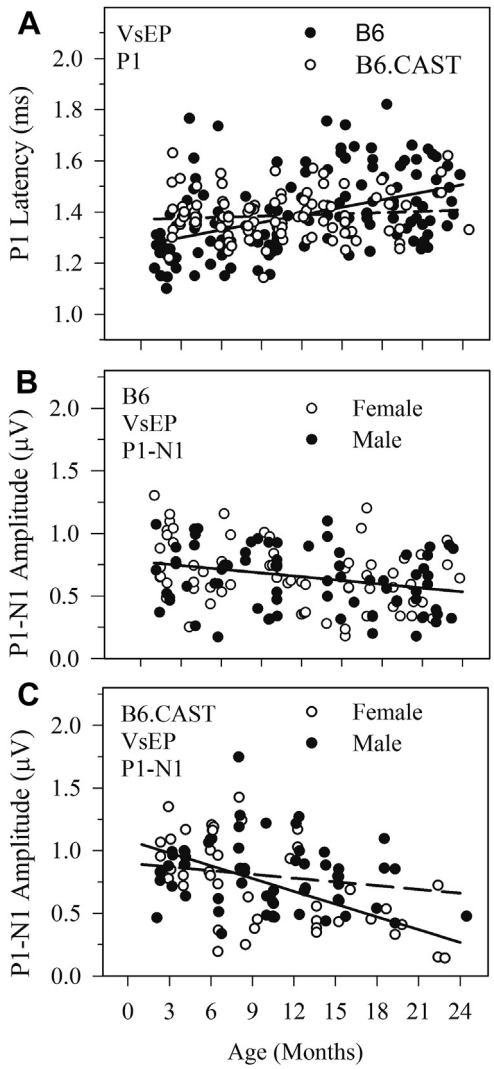

Fig. 3. VsEP latency and amplitude as a function of age for B6 and B6.CAST strains. (A) Combined male and female data for B6 (closed circles) and B6.CAST (open circles) strains. VsEP onset latency (P1) increased progressively as a function of age for B6. The rate of increase was quite modest. Regression equation for line shown: B6: y = 9.84x + 1270 (microseconds). The regression slope for B6.CAST data was not significant (p = 0.33); Line shown (dashed) for B6.CAST: y = 1.52x + 1371 (microseconds). (B) P1-N1 amplitudes decreased with age for B6 mice. There was no difference between males (filled circles) and females (open circles). Aging rate is based on combined male and female data: linear regression line shown: y = −0.010x + 0.775 (microvolts). (C) P1-N1 amplitudes decreased with age also for B6.CAST animals. Based on linear regression analysis however, male (filled circles) and females (open circles) B6.CAST appeared to age at different rates. Amplitudes decreased at a greater rate for female B6.CAST mice compared with both B6.CAST males and B6 mice. B6.CAST linear regression lines shown: Males: y = −0.010x + 0.90 (microvolts); Females: y = −0.034x + 1.08 (microvolts). Abbreviation: VsEP, vestibular sensory evoked potentials.

VsEP amplitudes (P1-N1) tended to decrease with age for both strains although the rate of decrease was relatively modest (Fig. 3B and 3C). There were no gender differences in age-related amplitude decline for B6 animals, and the slope for the combined data was −0.010 μV per month (Fig. 3B, intercept = 0.78 μV, F(1,137) = 13.159, $p = 4.03 \times 10^{-4}$; $R^2 = 0.088$). For B6.CAST mice (Fig. 3C), there was no general effect of gender on P1-N1 amplitudes when age was taken into consideration (ANOVA, age as covariate). However, the VsEP amplitude decline with age for B6.CAST females was more pronounced than that for males (Fig. 3C, females = −0.034 μV per month, males = −0.010 μV per month; Zar-*t*: $p < 0.05$). Although there was no difference in the rate of decline between B6 mice and male B6.CAST mice (Fig. 3C, B6.CAST slope = −0.010 μV per month, intercept = 0.9 μV, F(1,53)= 1.777, $p = 0.188$, $R^2 = 0.032$), female B6.CAST mice evidenced a steeper age-related decline than B6 animals (Zar-*t*: $p < 0.05$). These represent notable lifetime age-related amplitude losses on the order of 0.24 μV (B6 animals and B6.CAST males) to 0.8 μV (B6.CAST females).

3.3. Age-related changes in auditory function

Of the 150 B6 animals that were successfully tested over the ages of 1–24 months, 30% (n = 49) showed absent ABRs for 8-kHz stimulation. In the case of B6.CAST, 73 animals were tested over a similar age range (2–24 month-old) and only 5 animals evidenced absent ABRs for 8-kHz stimulation. Moreover, 8-kHz ABRs were absent in some B6 animals as early as 10 months, whereas absent responses appeared for the first time at about 17 months in B6.CAST mice. Fig. 4 illustrates the time course of acquiring absent ABRs in B6 animals compared to the time profile of B6.CAST animals. For B6, responses to the highest frequencies (32 and 41.2 kHz) were affected first (within 4–6 months), and by about 11 months, all animals failed to respond to high frequency stimuli. Loss of responses to 8 and 16 kHz appeared later (~10 months) with all animals failing to respond to 16 kHz stimuli at about 16 months and older. Eighty to 90% of animals had no responses to 8-kHz stimuli at ages above 18 month-old. These observations can be contrasted with results from B6.CAST animals (Fig. 4B). In this case, responses were present in all animals at all frequencies up to at least 18 months of age. At older ages, the fraction of animals with absent ABR increased but at most rose to about 50%.

Both strains evidenced progressive increases in ABR thresholds with increasing age (Fig. 2). However, the aging rates for 8-kHz ABR thresholds (regression slopes) were significantly steeper for B6 (slope = 4.22 dB per month, intercept = 23.387 dB peSPL, F(1, 139) = 391.694; $p = 2.867 \times 10^{-42}$, $R^2 = 0.762$) than those for B6.CAST (slope = 2.789 dB per month, intercept = 26.793 dB peSPL, F(1,71) =109.622, $p = 4.83 \times 10^{-16}$, $R^2 = 0.607$) mice (Zar-*t*: $p < 0.05$). Similar findings were observed for threshold aging rates at 16, 32, and 41.2 kHz, where rates were considerably steeper for B6 mice (Zar-*t*: $p < 0.05$). These findings confirm earlier reports (Keithley et al., 2004), extend findings to 41.2 kHz, and provide additional detail regarding the progressive nature of age-related hearing loss in the 2 strains.

3.4. Comparisons between gravity receptor and auditory functional aging

Although the sensitivity of gravity receptors decreased somewhat with age, the rate of decline in auditory function was substantially greater than that for vestibular function in both mouse strains (Zar-*t*: $p < 0.05$), and the difference between auditory and macular decline was more pronounced in the B6 strain. Functional

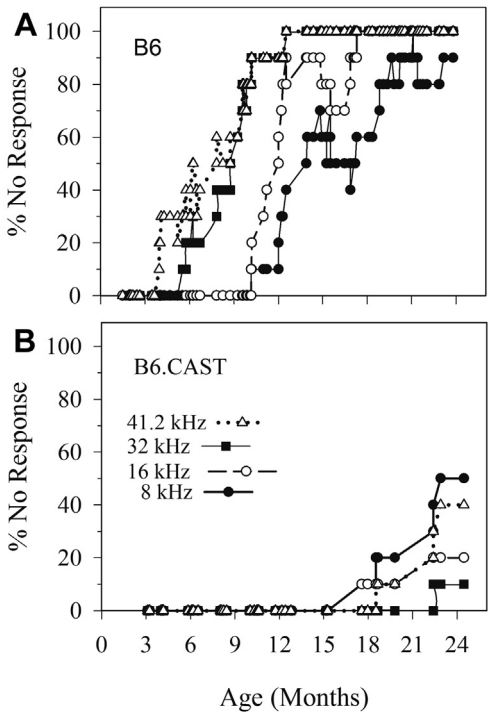

Fig. 4. Hearing loss profiles for B6 (A) and B6.CAST (B) mice based on ABR thresholds for 8, 16, 32, and 41.2-kHz stimuli. Graphs represent the % of animals having no response at the highest possible stimulus level for each frequency. Note that profound loss in B6 (A) begins as early as 3 months for 41.2 kHz, 6 months for 32 kHz, and 10 months for 16 and 8 kHz. Complete loss (no response in any animal tested, 100 %) appears in the highest frequencies (32 and 41.2 kHz) beginning at about 12 months and at 17 months for 16 kHz. Losses of 80%–90% for 8 kHz appear at about 19 months of age. In contrast, profound hearing loss does not begin to appear until approximately 18 months of age for B6.CAST and maximum deficits approach only 50% at the oldest ages. Abbreviation: ABR, auditory brainstem responses.

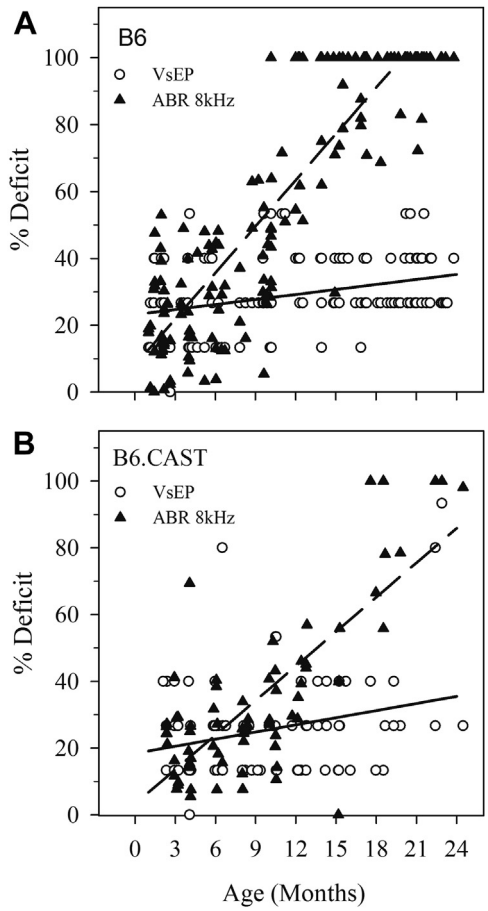

Fig. 5. Normalized thresholds showing percentage deficit of VsEP and 8-kHz ABR dynamic ranges as a function of age. The % deficit reflects the loss in sensory dynamic range because of elevated thresholds. Hundred percent indicates complete loss in dynamic range that is no response at any stimulus level. Combined male and female data for both strains are represented. (A) B6: percent deficit for VsEP thresholds (open circles) increased slightly with age. The average rate of decline is indicated by the regression line shown (solid): $y = 0.50x + 23.2\%$. In contrast, ABR percent deficit increased at a steep rate for B6 (dashed line): $y = 4.61x + 8.0\%$. (B) B6.CAST: Percent deficit increased slightly with age similar to B6 at an average rate shown by the regression line shown (solid): $y = 0.71 + 18.4\%$. Percent deficit for ABR in B6.CAST increased at a significantly higher rate than VsEP but at a significantly lower rate than B6 ABR. Regression line (dashed): $y = 3.44 + 3.3\%$. Abbreviations: ABR, auditory brainstem responses; VsEP, vestibular sensory evoked potentials.

deficit (fraction of normal dynamic range in %) ranged from 0% (no deficit) to 100% (complete loss of function as indicated by absent responses). On average, the loss in dynamic range for 8-kHz ABR increased at a rate of 4.61% per month for B6 mice and 3.44% per month for B6.CAST (Fig. 5A and B; Zar-*t*: $p < 0.05$), whereas the loss in VsEP dynamic range was only 0.50% per month and 0.71% per month for the B6 and B6.CAST, respectively, (Fig. 5).

3.5. Morphological changes in utricle

Morphometric data are shown in Figs. 6 and 7. There was no relationship between age and hair cell density, postsynaptic patch density or synaptic density (Fig. 7A, C and D). The only significant relationship found with age was a small increase in CtBP2 puncta density in B6 animals (slope = 0.21 puncta per hair cell per month; $p = 0.033$; $R^2 = 0.22$, Fig. 7B). However, these changes were small inasmuch as there was no significant difference in ribbon density between strains and there was no age-related change in ribbon density for B6.CAST animals. On average across ages, B6 epithelia had somewhat higher hair cell densities but lower synaptic densities per hair cell (Fig. 7A and B, Kruskal–Wallis, $p < 0.001$). There were no physiological correlates of these differences.

4. Discussion

The findings of the present study show that: (1) there is a very low rate of decline in vestibular sensitivity over the lifetime of B6 and B6.CAST mouse strains; (2) the vestibular functional aging profiles for the 2 strains were comparable, thus, the *Ahl* mutation had little or no substantial impact on gravity receptor aging; (3) vestibular and auditory receptor function declined at markedly different rates with age, both strains evidenced a substantially higher rate of decline in auditory function compared to vestibular; (4) auditory functional losses with age in B6 mice occurred earlier and were more severe than those expressed by B6.CAST mice, thus confirming earlier work (Keithley et al., 2004); and (5) there were no age-related changes in macular hair cell or synaptic densities for either strain. Although auditory and vestibular end organs are similar and linked physiologically in many important ways, the results of the present study clearly demonstrate that aging processes and rates of decline in the 2 sensory systems can be quite distinct and independent.

Virtually nothing is known about genes controlling normal vestibular aging. The present findings indicate that there may be some genetic basis for the long-lived vestibular stability in the B6 genome, (the genome common to both strains studied here). This is interesting given the fact that both auditory and vestibular epithelia

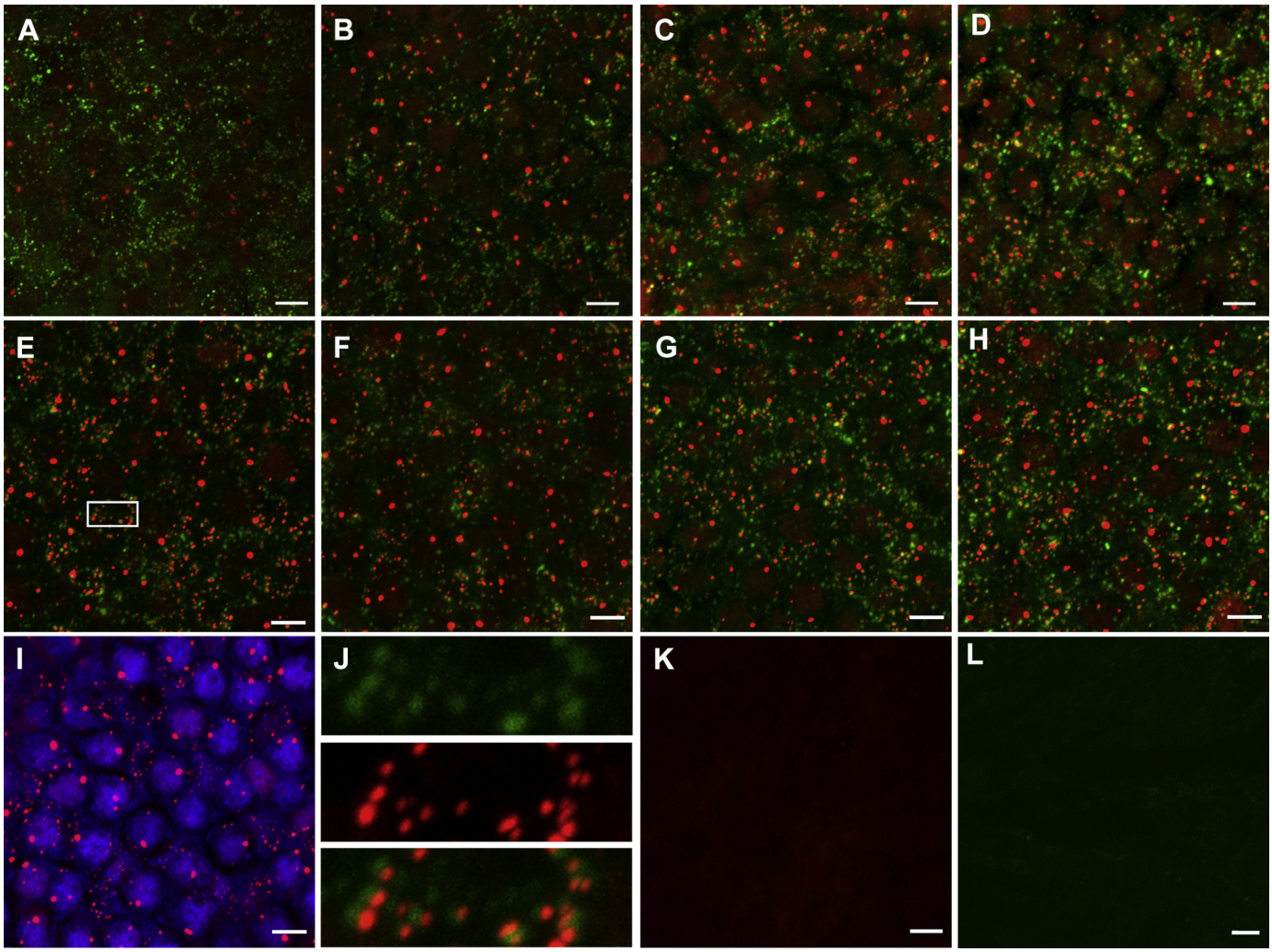

Fig. 6. Representative maximum intensity projections of *z*-stack images showing immunolabeled postsynaptic patches and the synaptic ribbon marker, CtBP2 in the utricular neuroepithelium of B6 (top row) and B6.CAST (middle row) mice of different age groups: B6 (A, B, C, and D), B6.CAST (E, F, G, and H). (I) Hair cell specific LHX3 immunolabeling (blue) co-localized with CtBP2 nuclear staining (red). Inset in (J) shows the co-localization of presynaptic ribbons (red) with postsynaptic patches (green). Preadsorption of SHANK1a and CtBP2 antibodies with their respective blocking peptides showed no immunolabeling (K and L). (Red, CtBP2 [C-terminal binding protein 2]; Green, SHANK1a [SH3 and multiple ankyrin repeat domains 1a]; Blue, LHX3 [LIM Homeobox 3], scale bar = 5 μm).

depend critically on *Cdh23* (Bolz et al., 2001; Bork et al., 2001; Di Palma et al., 2001a; Lagziel et al., 2005; Michel et al., 2005; Wilson et al., 2001), yet as shown here, changes in the gene product or available isoforms that are not complete functional nulls may favor one end organ over the other.

Null mutations of *Cdh23* produce striking developmental defects in vestibular and auditory stereociliary bundles, leading to profound hearing loss and to waltzer behaviors (i.e., circling, head bobbing and so forth; Di Palma et al., 2001a, 2001b; Lefevre et al., 2008; Wada et al., 2001; Wilson et al., 2001; Yonezawa et al., 2006). These null mutations of *Cdh23* are accompanied by profound vestibular functional loss (Jones et al., 2005; $Cdh23^{v-2J}$) and serve as models of human USH1 syndrome. In contrast, recently described non-null *Cdh23* missense mutations in mice such as *salsa* (Schwander et al., 2009), *jera* (Manji et al., 2011), and *erlong* (Han et al., 2012), present with profound hearing loss and normal behaviors and thus were offered as models of human DFNB12. Evidence from the *salsa* and *jera* strains showed that hearing loss was accompanied by the loss of stereociliary tip links after the onset of hearing, presumably because of the reduced ligand-binding adhesion strength shown by the altered *Cdh23* protein (Manji et al., 2011; Schwander et al., 2009). In the presence of Ca^{2+}, the proteins CDH23 and protocadherin 15 (PCDH15) are normally tightly bound together to form stereociliary tip link filaments, which are required to gate stereociliary mechanotransduction channels (e.g., Müller, 2008). Schwander et al. (2009) and Manji et al. (2011) argued that the weakened adhesive bonding strength of *Cdh23* in these mutants rendered tip links susceptible to mechanical damage during sound stimulation, and this led to profound hearing loss. Although vestibular function was not measured directly in any of these missense mouse strains, Schwander et al. speculated that low frequency vestibular mechanoreceptors had some unspecified different mechanical properties, and these were responsible for preserving vestibular sensors. Although vestibular tip links were reportedly present in *salsa* and *jera* strains, the actual extent to which vestibular function was spared in *salsa*, *jera*, and *erlong* strains remains to be determined. Our findings provide definitive direct evidence that vestibular function is spared throughout the lifespan of the B6 strain despite harboring the $Cdh23^{753A}$ mutation.

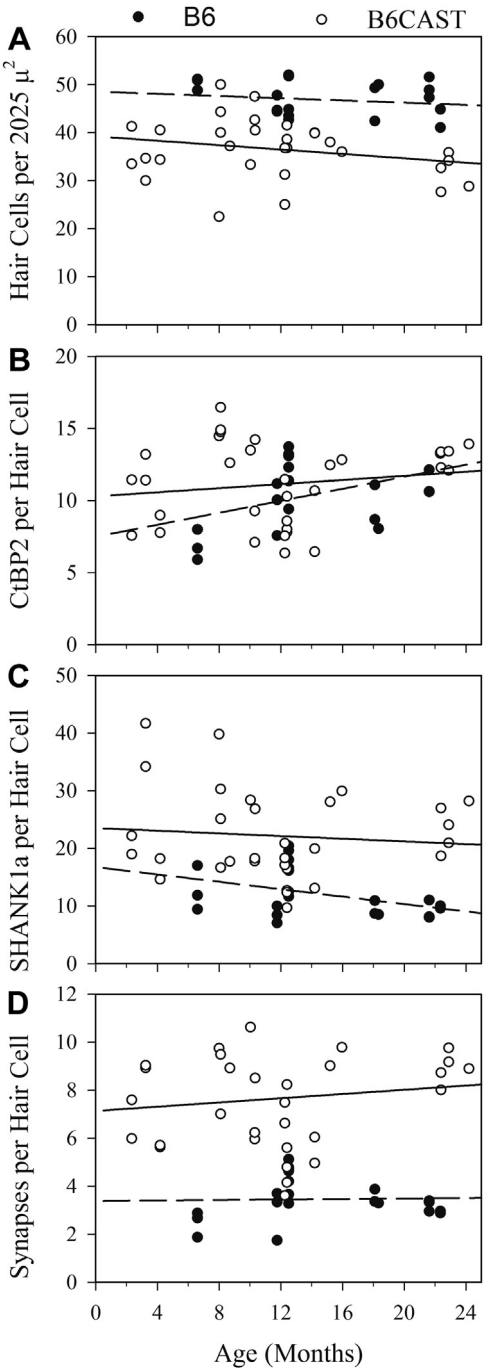

Fig. 7. Hair cells and synaptic elements in the utricular sensory epithelium of B6 and B6.CAST mice across age. Represented are counts of puncta from macular epithelial samples in B6 (filled symbols) and B6.CAST mice (open symbols). Regression lines for each metric are shown, dashed for B6, and solid for B6.CAST. Only 1 metric indicated a relationship to age. B6 CtBP2 density (B) evidenced a shallow but significant increase with age (slope = 0.208 puncta/month, intercept = 7.51, R^2 = 0.219, p = 0.033). No other slopes were significant. (A) Hair cell density: hair cell count per scan area of 2025 square microns. (B) Synaptic ribbon density: CtBP2 puncta per hair cell. (C) Postsynaptic patch density: SHANK1a puncta per hair cell. (D) Synaptic density: number of co-localized CtBP2 and SHANK1a puncta per hair cell. Abbreviations: CtBP2, C-terminal binding protein 2; SHANK1a, SH3 and multiple ankyrin repeat domains 1a.

The hypomorphic *Ahl* mutation ($Cdh23^{753A}$) studied here also results in altered Ca^{2+} binding regions in extracellular domains of the CDH23 protein, thus, the mutation also weakens adhesion and decreases the strength of CDH23 ligand binding (Noben-Trauth et al., 2003). One expects that the weak ligand bonds affect tip links, and this may contribute to ARHL and to the well-known predisposition for noise-induced hearing loss (NIHL) in *Ahl* mutant mice (e.g., Davis et al., 2001; Willott et al., 1998). Thus, there is general agreement among investigators that hypomorphic mutations in *Cdh23* lead to increased susceptibility to auditory damage during stimulation (e.g., NIHL), and this may include mechanical disruption and loss of tip links.

What mechanism is responsible for sparing vestibular but not cochlear function in *Ahl* mutants? The answer is not entirely clear. If we consider the forces operating at the stereociliary bundle during natural stimulation, we can argue *a priori* that peak forces driving bundle motion are proportional to peak acceleration (f = ma). For any given displacement, peak acceleration and hence peak force will be proportional to the square of the frequency. This suggests the possibility that bundles subjected to the highest frequencies would experience the highest forces and suffer the most damage. Such would produce a pattern of pathology like that found in ARHL and NIHL. This putative mechanism requires no special mechanical properties for vestibular mechanoreceptors. Gravity receptors in mice may be subject to stimulus frequencies at least up to about 300 Hz (Jones et al., 2015), whereas the cochlea experiences frequencies well above 50 kHz (Ehret, 1976). Forces associated with vestibular sensory stimulation therefore may be far less likely to produce damage to tip links and other bundle filaments containing the altered *Cdh23* product. This is true when the larger displacements anticipated for vestibular hair cell (HC) bundles (e.g., Géléoc et al., 1997) are taken into consideration. The loss of tip links may be exacerbated in cells prone to damage because of a potential reduction in the rate of tip link regeneration (Lelli et al., 2010). Cdh23 levels in the "readily available pool" (Lelli et al., 2010) could be significantly reduced owing to cellular targeting and destruction of abnormally folded $Cdh23^{753A}$ (Manji et al., 2011; Noben-Trauth et al., 2003).

The differential loss of tip links would clearly explain a profound hearing loss accompanied by normal vestibular function, however, alone it does not immediately explain the induction of apoptosis and massive loss of cochlear hair cells associated with ARHL and NIHL (Bao and Ohlemiller, 2010; Park et al., 2010; Someya and Prolla, 2010, Someya et al., 2009; Tadros et al., 2008; Wang et al., 2012; Xiong et al., 2015). The loss of reflex activation of olivocochlear inhibition, which would accompany loss of tip links, is an additional mechanism likely contributing to differential effects of the *Ahl* mutation on auditory and vestibular sensors. Evidence suggests that olivocochlear efferent inhibition of outer hair cell motility and reduction of primary afferent activity provides protection against NIHL (Darrow et al., 2007; Maison et al., 2002; Taranda et al., 2009). Loss of cochlear HC tip links would uncouple the afferent leg of the olivocochlear reflexes and lead to greater susceptibility to bundle, HC and primary afferent damage. Owing to the postsynaptic action and pattern of cochlear efferent innervation, loss of the reflex would also promote a basal to midcochlear progression of injury. No similar consequences would be anticipated for the vestibular system. Although vestibular efferents are present, when activated, the action of vestibular efferents on vestibular afferent activity in mammals is largely excitatory (Holt et al., 2011), and to our knowledge, no protective role is recognized.

There may be otherwise unknown molecular mechanism available to protect vestibular sensors. Elucidating the mechanisms underlying these differential functional effects of mutation is of considerable interest and is the target of future research.

Vestibular functional aging has now been studied in some detail in 4 inbred mouse strains including B6, B6.CAST, CBA/CaJ (Mock et al., 2011), and A/J (Vijayakumar et al., 2015). Among the 4 strains, B6 and B6.CAST show the lowest rates of decline in macular

threshold with age corresponding to an increase in threshold of less than 3 dB over 24 months. The rate of vestibular aging in CBA mice is 3 times higher than that of B6.CAST and over 4 times higher than B6. The A/J inbred mouse evidences vestibular threshold aging rates lower than CBA but greater than B6 and B6.CAST. These findings clearly suggest that vestibular aging in inbred mice depends on gene variation across strains. It will be important to begin identifying and exploring genes mediating age-related vestibular loss, and this will likely be facilitated with the use of well-characterized inbred mouse strains.

The effect of gender on the vestibular system is poorly understood. A search of the literature reveals no reports of gender differences in vestibular structures or function in relation to aging in mice. Results from the present study suggest that there are no gender differences in macular sensitivity or in the rate of change in macular sensitivity for either strain across age. Gender differences in auditory function have been reported in B6 mice (Henry, 2004), wherein male B6 mice reportedly had more sensitive hearing and lost hearing later than females. Results of the present study confirm higher thresholds for females generally across age for 8 and 16-kHz ABRs. We did not find different aging rates for males and females as one might anticipate based on Henry's report. Nonetheless, the generally higher thresholds observed for females may be seen to contribute to an earlier appearance of profound hearing loss.

The findings of Johnson et al. (2010) and the present results indicate minimal changes in vestibular hair cell density with age, whereas Shiga et al. (2005) and Park et al. (1987) reported mild decreases in hair cell density in vestibular end organs of B6 mice. Park et al. showed that between the ages of 1-month to about 30 months of age, hair cell density declined by 14% in the utricle, 19% in the saccule, and 19%–24% in ampullar cristae. The present study showed no changes in hair cell or synaptic density out to 24 months. Clearly, the vestibular epithelium failed to show the major changes evidenced by cochlear sensory elements in ARHL. Our findings are consistent with a small progressive decline in the vestibular epithelium of B6 and B6.CAST mice that is not accompanied by substantial structural loss. From the present results it is clear that the modest decline in vestibular function is unrelated to the *Ahl* mutation.

Differences in the aging profiles for VsEP latencies and amplitudes were noted for B6 and B6.CAST animals. B6.CAST animals showed little or no appreciable increase in latency with age, whereas B6 latencies increased at a slow rate of about 10 μs per month with lifetime increases on the order of 240 μs, thus representing modest latency shifts only in old-age. VsEP amplitudes decreased with age for both strains although the B6.CAST rate of decline was greater than B6 mice, but only for B6.CAST females. Although we cannot rule out a role for *Ahl* in these observed minor differences between strains, we can in any case underscore the fact that the scale of effects in the vestibular organs is negligible compared to those in the cochlea.

Establishing aging profiles for many different inbred mouse strains is 1 strategy for identifying new gene variants that influence age-related declines in vestibular function inasmuch as differences found among strains may suggest a genetic basis. Examining many new strains will improve the context available for making such comparisons and facilitate the identification of candidate gene variants.

Disclosure statement

The authors declare that there are no actual or potential conflicts of interest associated with this work and publication.

Acknowledgements

The authors would like to thank Dr. Samuel L Pfaff (Salk Institute, La Jolla, CA) for the generous gift of LHX3 antibody. The authors also thank the following students and lab technicians for their help in collecting and processing data as well as assistance with various other aspects of this project: Fiona Foley, Stacy Harrison, Jack Hill, Chris Gaines, Kristal Mills, Candice Manning, Elizabeth Croskery, Leonardo Duque, Taylor Boney, Chad Bailey, and Alan Kunz. This research was supported by NIDCD F31 DC008012 (BEM), NIH RO1 DC 006443 (SMJ), and an American Academy of Audiology Student Investigator Research Award (BEM).

References

Baloh, R.W., Jacobson, K.M., Socotch, T.M., 1993. The effect of aging on visual-vestibuloocular responses. Exp. Brain Res. 95, 509–516.
Bao, J., Ohlemiller, K.K., 2010. Age-related loss of spiral ganglion neurons. Hear Res. 264, 93–97.
Bartolomé, M.V., del, C.E., López, L.M., Carricondo, F., Poch-Broto, J., Gil-Loyzaga, P., 2002. Effects of aging on C57BL/6J mice: an electrophysiological and morphological study. Adv. Otorhinolaryngol. 59, 106–111.
Bolz, H., Brederlow, B., Ramirez, A., Bryda, E.C., Kutsche, K., Nothwang, H.G., Seeliger, M., del C-Salcedó Cabrera, M., Vila, M.C., Molina, O.P., Gal, A., Kubisch, C., 2001. Mutation of Cdh23, encoding a new member of the cadherin gene family, causes Usher syndrome type 1D. Nat. Genet. 27, 108–112.
Bork, J.M., Peters, L.M., Riazuddin, S., Bernstein, S.L., Ahmed, Z.M., Ness, S.L., Polomeno, R., Ramesh, A., Schloss, M., Srisailpathy, C.R., Wayne, S., Bellman, S., Desmukh, D., Ahmed, Z., Khan, S.N., Kaloustian, V.M., Li, X.C., Lalwani, A., Riazuddin, S., Bitner-Glindzicz, M., Nance, W.E., Liu, X.Z., Wistow, G., Smith, R.J., Griffith, A.J., Wilcox, E.R., Friedman, T.B., Morell, R.J., 2001. Usher syndrome 1D and nonsyndromic autosomal recessive deafness DFNB12 are caused by allelic mutations of the novel cadherin-like gene Cdh23. Am. J. Hum. Genet. 68, 26–37.
Braude, J.P., Vijayakumar, S., Baumgarner, K., Laurine, R., Jones, T.A., Jones, S.M., Pyott, S.J., 2015. Deletion of Shank1 has minimal effects on the molecular composition and function of glutamatergic afferent postsynapses in the mouse inner ear. Hear Res. 321, 52–64.
Colledge, N.R., Wilson, J.A., Macintyre, C.C., MacLennan, W.J., 1994. The prevalence and characteristics of dizziness in an elderly community. Age Ageing 23, 117–120.
Darrow, K.N., Maison, S.F., Liberman, M.C., 2007. Selective removal of lateral olivocochlear efferents increases vulnerability to acute acoustic injury. J. Neurophsiol. 97, 1775–1785.
Davis, R.R., Newlander, J.K., Ling, X.-B., Cortopassi, G.A., Krieg, E.F., Erway, L.C., 2001. Genetic basis for susceptibility to noise-induced hearing loss in mice. Hear Res. 155, 82–90.
Di Palma, F., Holme, R.H., Bryda, E.C., Belyantseva, I.A., Pellegrino, R., Kachar, B., Steel, K.P., Noben-Trauth, K., 2001a. Mutations in *Cdh23*, encoding a new type of cadherin, cause stereocilia disorganization in waltzer, the mouse model for Usher synsrom type 1D. Nat. Genet. 27, 103–107.
Di Palma, F., Pellegrino, R., Noben-Trauth, K., 2001b. Genomic structure, alternative splice forms and normal and mutant alleles of cadherin 23 (Cdh23). Gene 281, 31–41.
Ehret, G., 1976. Development of absolute auditory thresholds in the house mouse (mus musculus). J. Am. Audiol. Soc. 1, 179–184.
Enrietto, A.J., Jacobson, K.M., Baloh, R.W., 1999. Aging effects on auditory and vestibular responses: a longitudinal study. Am. J. Otolaryngol. 20, 371–378.
Furman, J.M., Redfern, M.S., 2001. Effect of aging on the otolith-ocular reflex. J. Vestib. Res. 11, 91–103.
Géléoc, G.S.G., Lennan, G.W.T., Richardson, G.P., Kros, C.J., 1997. A quantitative comparison of mechanoelectrical transduction in vestibular and auditory hair cells of neonatal mice. Proc. R. Soc. Lond. B 264, 611–621.
Goebel, J.A., 2001. Practical management of the dizzy patient. Lippincott, Williams & Wilkins, Philadelphia.
Gorlin, R.J., Toriello, H.V., Cohen, M.M. (Eds.), 1995. Hereditary hearing loss and its syndromes. Oxford University Press, New York.
Han, F., Yu, H., Tian, C., Chen, H.E., Benedict-Alderfer, C., Whend, Y., Wnag, Q., Han, X., Zheng, Y., 2012. Early-onset hearing loss facilitates evaluation of otoprotection drugs. Pharmacogenomics J. 12, 30–44.
Henry, K.R., 2002. Sex- and age-related elevation of cochlear nerve envelope response (CNER) and auditory brainstem response (ABR) thresholds in C57BL/6 mice. Hear Res. 170, 107–115.
Henry, K.R., 2004. Males lose hearing earlier in mouse models of late-onset age-related hearing loss; females lose hearing earlier in mouse models of early-onset hearing loss. Hear Res. 190, 141–148.
Hequembourg, S., Liberman, M.C., 2001. Spiral ligament pathology: a major aspect of-age-related cochlear degeneration in C57BL/6 mice. J. Assoc. Res. Otolaryngol. 2, 118–129.
Hoffman, H.J., Sklare, D.A., 2003. Vestibular system problems: righting the balance. Assoc. Res. Otolaryngol. Abst. 26, 133.

Holt, J.C., Lysakowski, A., Goldberg, J.M., 2011. The efferent vestibular system. In: Ryugo, D.D., Fay, R.R., Popper, A.N. (Eds.), Auditory and Vestibular Efferents. Springer, New York, pp. 135–186.
Hume, C.R., Bratt, D.L., Oesterle, E.C., 2007. Expression of LHX3 and SOX2 during mouse inner ear development. Gene Expr. Patterns 7, 798–807.
Johnson, K.R., Erway, L.C., Cook, S.A., Willott, J.F., Zheng, Q.Y., 1997. A major gene affecting age-related hearing loss in C57BL/6J mice. Hear Res. 114, 83–92.
Johnson, K.R., Yu, H., Ding, D., Jiang, H., Gagnon, L.H., Salvi, R.J., 2010. Separate and combined effects of *Sod1* and *Cdh23* mutations on age-related hearing loss and cochlear pathology in C57BL/6J mice. Hear Res. 268, 85–92.
Jones, S.M., Johnson, K.R., Yu, H., Erway, L.C., Alagramam, K.N., Pollak, N., Jones, T.A., 2005. A quantitative survey of gravity receptor function in mutant mouse strains. J. Assoc. Res. Otolaryngol. 6, 297–310.
Jones, S.M., Jones, T.A., Johnson, K.R., Yu, H., Erway, L.C., Zheng, Q.Y., 2006. A comparison of vestibular and auditory phenotypes in inbred mouse strains. Brain Res. 1091, 40–46.
Jones, T.A., Lee, C., Gaines, G.C., Grant, J.W., 2015. On the high frequency transfer of mechanical stimuli from the surface of the head to the macular neuroepithelium of the mouse. J. Assoc. Res. Otolaryngol. 16, 189–204.
Kazmierczak, P., Sakaguchi, H., Tokita, J., Wilson-Kubalek, E.M., Milligan, R.A., Muller, U., Kachar, B., 2007. Cadherin 23 and protocadherin 15 interact to form tip-link filaments in sensory hair cells. Nature 449, 87–92.
Keithley, E.M., Canto, C., Zheng, Q.Y., Fischel-Ghodsian, N., Johnson, K.R., 2004. Age-related hearing loss and the ahl locus in mice. Hear Res. 188, 21–28.
Khimich, D., Nouvian, R., Pujol, R., Tom Dieck, S., Egner, A., Gundelfinger, E.D., Moser, T., 2005. Hair cell synaptic ribbons are essential for synchronous auditory signalling. Nature 434, 889–894.
Lagziel, A., Ahmed, Z.M., Schultz, J.M., Morell, R.J., Belyantseva, I.A., Friedman, T.B., 2005. Spatiotemporal pattern and isoforms of cadherin 23 in wild type and waltzer mice during inner ear hair cell development. Dev. Biol. 280, 295–306.
Latoche, J.R., Neely, H.R., Noben-Trauth, K., 2011. Polygenic inheritance of sensorineural hearing loss (Snhl2, -3, and -4) and organ of Corti patterning defect in the ALR/LtJ mouse strain. Hear Res. 275, 150–159.
Lee, S.I., Conrad, T., Jones, S.M., Lagziel, A., Starost, A.F., Belyantseva, I., Friedman, T.B., Morell, R.J., 2013. A null mutation of mouse *Kcna10* causes significant vestibular and mild hearing dysfunction. Hear Res. 300, 1–9.
Lefèvre, G., Michel, V., Weil, D., Lepelletier, L., Bizard, E., Wolfrum, U., Hardelin, J.P., Petit, C., 2008. A core cochlear phenotype in USH1 mouse mutants implicates fibrous links of the hair bundle in its cohesion, orientation and differential growth. Development 135, 1427–1437.
Lelli, A., Kazmierczak, P., Kawashima, Y., Müller, U., Holt, J.R., 2010. Development and regeneration of sensory transduction in auditory hair cells requires functional interaction between Cadherin-23 and Protocadherin-15. J. Neurosci. 30, 11259–11269.
Liberman, L.D., Wang, H., Liberman, M.C., 2011. Opposing gradients of ribbon size and AMPA receptor expression underlie sensitivity differences among cochlear-nerve/hair-cell synapses. J. Neurosci. 31, 801–808.
Maison, S.F., Luebke, A.E., Lieberman, M.C., Zuo, J., 2002. Efferent protection from acoustic injury is mediated via alpha 9 nicotinic acetylcholine receptors on outer hair cells. J. Neurosci. 22, 10838–10846.
Manji, S.S.M., Miller, K.A., Williams, L.H., Andreasen, L., Siboe, M., Rose, E., Bahlo, M., Kuiper, M., Dahl, H.H., 2011. Molecular pathogenesis of genetic and inherited diseases an ENU-induced mutation of Cdh23 causes congenital hearing loss, but no vestibular dysfunction, in mice. Am. J. Pathol. 179, 903–914.
McFadden, S.L., Ding, D., Salvi, R., 2001. Anatomical, metabolic and genetic aspects of age-related hearing loss in mice. Audiology 40, 313–321.
Mendus, D., Sundaresan, S., Grillet, N., Wangsawihardja, F., Leu, R., Müller, U., Jones, S.M., Mustapha, M., 2014. Thrombospondins 1 and 2 are important for afferent synapse formation and function in the inner ear. Eur. J. Neurosci. 39, 1256–1267.
Michel, V., Goodyear, R.J., Weil, D., Marcotti, W., Perfettini, I., Wolfrum, U., Kros, C.J., Richardson, G.P., Petit, C., 2005. Cadherin 23 is a component of the transient lateral links in the developing hair bundles of cochlear sensory cells. Dev. Biol. 280, 281–294.
Mock, B., 2008. Functional aging of the inner ear sensory systems in mouse models of age-related hearing loss. Dissertation. East Carolina University, Greenville, NC.
Mock, B., Jones, T.A., Jones, S.M., 2011. Gravity receptor aging in the CBA/CaJ strain: a comparison to auditory aging. J. Assoc. Res. Otolaryngol. 12, 173–183.
Morton, N.E., 1991. Genetic epidemiology of hearing impairment. Ann. N. Y. Acad. Sci. 630, 16–31.
Müller, U., 2008. Cadherins and mechanotransduction by hair cells. Curr. Opin. Cell Biol. 20, 557–566.
Nazareth, A.M., Jones, T.A., 1998. Central and peripheral components of short latency vestibular responses in the chicken. J. Vestib. Res. 8, 233–252.
Noben-Trauth, K., Johnson, K.R., 2009. Inheritance patterns of progressive hearing loss in laboratory strains of mice. Brain Res. 1277, 42–51.
Noben-Trauth, K., Zheng, Q.Y., Johnson, K.R., 2003. Association of Cadherin23 with polygenic inheritance and genetic modification of sensorineural hearing loss. Nat. Genet. 35, 21–23.
Paige, G.D., 1992. Senescence of human visual-vestibular interactions. 1. Vestibulo-ocular reflex and adaptive plasticity with aging. J. Vestib. Res. 2, 133–151.
Paige, G.D., 1994. Senescence of human visual-vestibular interactions: smooth pursuit, optokinetic, and vestibular control of eye movements with aging. Exp. Brain Res. 98, 355–372.
Park, J.C., Hubel, S.B., Woods, A.D., 1987. Morphometric analysis and fine structure of the vestibular epithelium of aged C57BL/6NNia mice. Hear Res. 28, 87–96.
Park, S.N., Back, S.A., Park, K.H., Kim, D.K., Park, S.Y., Oh, J.H., Park, Y.S., Yeo, S.W., 2010. Comparison of cochlear morphology and apoptosis in mouse models of presbycusis. Clin. Exp. Otorhinolaryngol. 3, 126–135.
Sage, C., Huang, M., Karimi, K., Gutierrez, G., Vollrath, M.A., Zhang, D.S., García-Añoveros, J., Hinds, P.W., Corwin, J.T., Corey, D.P., Chen, Z.Y., 2005. Proliferation of functional hair cells in vivo in the absence of the retinoblastoma protein. Science 307, 1114–1118.
Schwander, M., Xiong, W., Tokita, J., Lelli, A., Elledge, H.M., Kazmierczak, P., Sczaniecka, A., Kolatkar, A., Wiltshire, T., Kuhn, P., Holt, J.R., Kachar, B., Tarantino, L., Müller, U., 2009. A mouse model for nonsyndromic deafness (DFNB2) links hearing loss to defects in tip links of mechanosensory hair cells. Proc. Natl. Acad. Sci. U. S. A. 106, 5252–5257.
Shiga, A., Nakagawa, T., Nakayama, M., Endo, T., Iguchi, F., Kim, T.S., Naito, Y., Ito, J., 2005. Aging effects on vestibulo-ocular responses in C57BL/6 mice: comparison with alteration in auditory function. Audiol. Neurootol. 10, 97–104.
Siemens, J., Lillo, C., Dumont, R.A., Reynolds, A., Williams, D.S., Gillespie, P.G., Müller, U., 2004. Cadherin 23 is a component of the tip link in hair-cell stereocilia. Nature 428, 950–955.
Söllner, C., Rauch, G.J., Siemens, J., Geisler, R., Schuster, S.C., Müller, U., Nicolson, Tl, 2004. Mutations in cadherin 23 affect tip links in zebra fish sensory hair cells. Nature 428, 955–999.
Someya, S., Prolla, T.A., 2010. Mitochondrial oxidative damage and apoptosis inage-related hearing loss. Mech. Ageing Dev. 131, 480–486.
Someya, S., Xu, J., Kondo, K., Ding, D., Salvi, R.J., Yamasoba, T., Rabinovitch, P.S., Weindruch, R., Leeuwenburgh, C., Tanokura, M., Prolla, T.A., 2009. Age-related hearing loss in C57BL/6J mice is mediated by Bak-dependent mitochondrial apoptosis. Proc. Natl. Acad. Sci. U. S. A. 106, 19432–19437.
Spongr, V.P., Flood, D.G., Frisina, R.D., Salvi, R.J., 1997. Quantitative measures of hair cell loss in CBA and C57BL/6 mice throughout their life spans. J. Acoust. Soc. Am. 101, 3546–3553.
Tadros, S.F., D'Souza, M., Zhu, X., Frisina, R.D., 2008. Apoptosis-related genes change their expression with age and hearing loss in the mouse cochlea. Apoptosis 13, 1303–1321.
Taranda, J., Maison, S.F., Ballestero, J.A., Katz, E., Savino, J., Vetter, D.E., Boulter, J., Liberman, M.C., Fuchs, P.A., Elgoyhen, A.B., 2009. A point mutation in the hair cell nicotinic cholinergic receptor prolongs cochlear inhibition and enhances noise protection. PLoS Biol. 7, 71–83.
Tinetti, M.E., Williams, C.S., Gill, T.M., 2000. Dizziness among older adults: a possible geriatric syndrome. Ann. Intern. Med. 132, 337–344.
Vijayakumar, S., Lever, T.E., Pierce, J., Zhao, X., Bergstrom, D., Lundberg, Y.W., Jones, T.A., Jones, S.M., 2015. Vestibular dysfunction, altered macular structure and trait localization in A/J inbred mice. Mamm. Genome 26, 154–172.
Wada, T., Wakabayashi, Y., Takahashi, S., Ushiki, T., Kikkawa, Y., Yonekawa, H., Kominami, R., 2001. A point mutation in a cadherin gene, Cdh23, causes deafness in a novel mutant, waltzer mouse niigata. Biochem. Biophys. Res. Commun. 83, 113–117.
Wang, Y., Chu, H., Zhou, L., Gao, H., Xiong, H., Chen, Q., Chen, J., Huang, X., Cui, Y., 2012. Correlation of PDCD5 and apoptosis in hair cells and spiral ganglion neurons of different age of C57BL/6J mice. J. Huazhong Univ. Sci. Technolog. Med. Sci. 32, 113–118.
Willott, J.F., Turner, J.G., Carlson, S., Ding, D., Seegers Bross, L., Falls, W.A., 1998. The BALB/c mouse as an animal model for progressive sensorineural hearing loss. Hear Res. 115, 162–174.
Wilson, S.M., Householder, D.B., Coppola, V., Tessarollo, L., Fritzsch, B., Lee, E.C., Goss, D., Carlson, G.A., Copeland, N.G., Jenkins, N.A., 2001. Mutations in Cdh23 cause nonsyndromic hearing loss in waltzer mice. Genomics 74, 228–233.
Xiong, H., Pang, J., Yang, H., Dai, M., Liu, Y., Ou, Y., Huang, Q., Chen, S., Zhang, Z., Xu, Y., Lai, L., Zheng, Y., 2015. Activation of miR-34a/SIRT1/p53 signaling contributes to cochlear hair cell apoptosis: implications for age-related hearing loss. Neurobiol. Aging 36, 1692–1701.
Yonezawa, S., Yoshizaki, N., Kageyama, T., Takahashi, T., Sano, M., Tokita, Y., Masaki, S., Inaguma, Y., Hanai, A., Sakurai, N., Yoshiki, A., Kusakabe, M., Moriyama, A., Nakayama, A., 2006. Fates of Cdh23/CDH23 with mutations affecting the cytoplasmic region. Hum. Mutat. 27, 88–97.
Zar, J.H., 1984. Biostatistical Analysis, second ed. Prentice Hall Inc, Englewood Cliff, NJ.
Zhao, X., Jones, S.M., Yamoah, E.N., Lundberg, Y.W., 2008. Otoconin-90 deletion leads to imbalance but normal hearing: a comparison with other otoconia mutants. Neuroscience 153, 289–299.